ECS Transactions, 25 (1) 757-764 (2009)
10.1149/1.3210627 ©The Electrochemical Society

High Temperature Operation of Direct Ethanol Fuel Cells with Nafion-TiO_2 Membranes and PtSn/C Electrocatalysts

R.A. Isidoro[a], B.R. Matos[a], M.A. Dresch[a], E.V. Spinacé[a], M. Linardi[a], E. Traversa[b] , F.C. Fonseca[a] , and E.I. Santiago[a].

[a] Energy and Nuclear Research Institute, 05508-000, São Paulo, Brazil
[b] International Center for Materials Nanoarchitectonics (MANA), National Institute for Materials Science (NIMS), 1-1 Namiki, Tsukuba, Ibaraki 305-0044, Japan

In this study, both PtSn/C electrocatalysts and composites electrolytes based on Nafion and mesoporous titania (Nafion-TiO_2) were evaluated in direct ethanol fuel cell operating at 130°C. PtSn/C catalysts with different compositions were prepared by alcohol-reduction process. The electrochemical activity of these electrocatalysts was verified by cyclic voltammetry and chronoamperometry measurements. Cast Nafion-TiO_2 composites were characterized by differential scanning calorimetry and *ac* impedance spectroscopy. The water uptake of the composites was determined by gravimetry. Membrane electrode assemblies composed by Nafion-TiO_2 electrolyte and PtSn/C anode were evaluate in DEFC operating in 80-130°C temperature range. Polarization curves showed an enhanced performance (maximum power density of ~50 mW cm^{-2}) for DEFC using combined PtSn/C (60:40) electrocatalyst and Nafion-TiO_2 (10 wt%) operating at 130°C.

Introduction

Proton exchange membrane fuel cell (PEMFC) has been envisioned as a promising electrical supply for portable, vehicular, and stationary applications. However, problems associated with production, management, storage, and distribution of the gaseous hydrogen stimulate the search of alternative fuels. Among potentially alternative fuels, methanol and ethanol have been widely investigated. Such fuels form a new class of PEMFC referred as Direct Alcohol Fuel Cell (DAFC), in which power density is provided by the direct alcohol oxidation (1).

Ethanol has been considered as a promising fuel for DAFC due to its lower toxicity when compared to methanol, renewability, environmental friendliness, and large-scale production (2). Although the complete oxidation of one ethanol molecule involves 12 electrons, this reaction is usually limited to 4 electrons in low temperature fuel cell, resulting in the formation of acetaldehyde and acetic acid intermediates. The incomplete oxidation is related to the difficulty of C-C bond cleavage in the ethanol molecule (3). Another inconvenience associated with the use of alcohol is the crossover effect that promotes the adsorption of the fuel and its intermediates onto the cathode, diminishing the oxygen reduction reaction (ORR) rate. Both effects provide a substantial loss of the overall performance of DEFC at low temperatures (4). In this context, the developments for the DEFC technology are mostly concerned to overcome both the fuel crossover and the incomplete oxidation of ethanol.

Several studies have been devoted to the development of electrocatalysts for DEFC based on platinum and oxophilic elements, mainly PtRu and PtSn (5-8) aiming at the electrooxidation of ethanol and/or its intermediates (CO-like species) at lower potentials when compared to Pt. Such effect is achieved by two mechanisms: i) a spillover process involving OH-species formed on the oxophilic sites (bifunctional mechanism) or ii) by formation of Pt alloy leading to a weakening of Pt-adsorbed species due to an electronic effect introduced by the second element (9).

Another possibility to improve the performance of PEMFC is the increase of the operation temperature. In general, the benefits of the fuel cells working at high temperatures are: acceleration the electrode reactions kinetics, enhanced CO tolerance, and facilitated water and heat managements (10). However, the operation temperature on PEMFC is limited to ~85^{o}C due to the strong dependence of the protonic transport of the absorbed water by the state-of-the-art Nafion electrolyte. As a result, Nafion exhibits a drastic decrease of the proton conductivity at temperatures close to the one of water evaporation (11). Organic-inorganic membranes based on both Nafion and inorganic components with hygroscopic properties, such as TiO_2 (12,13), SiO_2 (14,15), and ZrO_2 (16), have been considered promising alternative to optimize the physical-chemistry properties of the conventional Nafion at high temperatures (100 - 140^{o}C) (17). The presence of the oxide phases contributes to the enhancement of the PEMFC performance due to the high water retention capacity and better transport properties. Moreover, in the DAFC case, the hindering of the transport of the alcohol through the organic-inorganic membranes results in a reduction of the fuel crossover.

In the context, the goal of the present study is to evaluate the performance of DEFC operating at high temperatures (130^{o}C) using Nafion- mesoporous TiO_2 composite electrolytes and PtSn/C eletrocatalysts prepared by an alcohol-reduction process.

Experimental

Nafion-mesoporous TiO_2 composite membranes having x=0 to 15 wt% of TiO_2 were prepared by casting. Initially, a commercial Nafion 5% solution (DuPont) was evaporated at ~80 °C and redissolved in dimethylsulfoxide (DMSO, Aldrich PA) under magnetic stirring. Mesoporous TiO_2 particles corresponding to the desired weight fraction of the inorganic phase were dispersed in DMSO by ultrasonic bath for 1 h and then added to the Nafion solution. The resulting solution was further homogenized in ultrasound for 30 min followed by magnetic stirring for 24 h. The membranes were cast by pouring the Nafion-TiO_2 solution in a teflon mold and heat treated at increasing temperature from 80 °C to 160 °C with 2 h of dwell time at each temperature as described elsewhere (18). Pure Nafion membranes were cast following the same thermal profile. The resulting membranes were cleaned and activated by heating in H_2O at 80 °C / 1 h, followed by consecutive treatments at 80 °C / 1 h in 7 mol L^{-1} HNO_3, H_2O_2, and H_2SO_4 , with intercalated treatments with H_2O and a final step of successive washings with H_2O until a pH = 7 was reached.

The water uptake capacity of the composite membranes was determined by the difference between dried and wet mass obtained after heat treatment at 110^{o}C/ 3h and immersion in hot water (80^{o}C/ 1h), respectively. Differential scanning calorimetry (DSC) data were obtained using an equipment Mettler/Toledo in the temperature range of -50 and 200^{o}C with heating rate of 20^{o}C min^{-1}. The transport properties of the samples were studied by two-probe electrochemical impedance spectroscopy (EIS) measurements, using a Solartron 1260 frequency analyzer, in the 100 Hz - 1 MHz frequency range and

applied amplitude of 200 mV. Impedance spectroscopy data were collected in the 25 °C - 80 °C temperature range with relative humidity (RH) ~ 98% in a home-made sample holder with Pt leads and a type-K thermocouple.

Electrocatalysts based on PtSn/C with different atomic ratios were prepared by an alcohol-reduction process (19). In this methodology, platinum and tin precursors (chloroplatinic acid 6-hydrate and tin chloride, Aldrich), ethylene glycol, and carbon (Vulcan XC-72) were kept in reflux for 3 h. The electrocatalysts were washed with water and dried at 75°C for 24 h. The electrochemical activity of the electrocatalysts was evaluated by cyclic voltammetry and chronoamperometry measurements (Autolab, PGSTAT 302N), using an ultrathin layer based on PtSn/C on glassy carbon disk electrode (0.196 cm^{-2}) and metal loading of 28μg cm^{-2} as working electrode as described elsewhere (20). Cyclic voltammetry experiments were performed in potential range of 0.1- 0.8V vs. ERH, and sweep rate of 20 mV s^{-1}. Chronoamperometry measurements were conducted in the presence of 1.0 mol L^{-1} ethanol solution at constant potential of 500 mV. All experiments were made in 0.5 mol L^{-1} H_2SO_4 electrolyte saturated with N_2.

Finally, both Nafion-mesoporous TiO_2 membranes and PtSn/C electrocatalysts were evaluated in a 5 cm^2 single fuel cells fed with ethanol solution (2mol L^{-1}, 2mL min^{-1}) in the anode and pure oxygen in the cathode with cell temperature and oxygen humidifier heated at 80°C and 130°C. The anode temperature was kept at room temperature (25°C) and atmospheric pressure (1 atm). The absolute oxygen pressure was 3 atm. The Pt and Nafion loadings were 1 mg cm^{-2} and 30 wt%, respectively, for both anode and cathode.

Results and Discussion

Fig. 1 shows the water uptake capacities for Nafion 115 and Nafion-TiO_2 composites as a function of the TiO_2 content. Cast Nafion presents a higher water uptake (~42%) than that observed for Nafion 115, which might be associated with higher isotropy of cast materials (21). However, the water uptake of composites slightly decreases with the increase of the TiO_2 content.

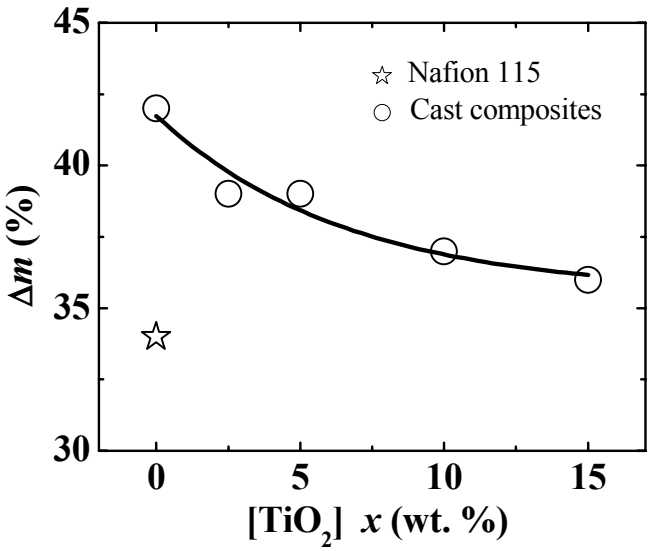

Figure 1: Water uptake as a function of TiO_2 content.

Fig. 2 shows Arrhenius plots for cast Nafion-TiO_2 composites with different TiO_2 contents. The experimental data evidenced a slightly decrease of the ionic conductivity for the composites with up to 10 wt% TiO_2, indicating that the presence of the insulating phase, in this concentration range, does not affect significantly the ohmic drop overpotential. Moreover, all studied samples exhibited a thermally activated proton transport with activation energy close to the one previously reported for Nafion (~0.1 eV) (18).

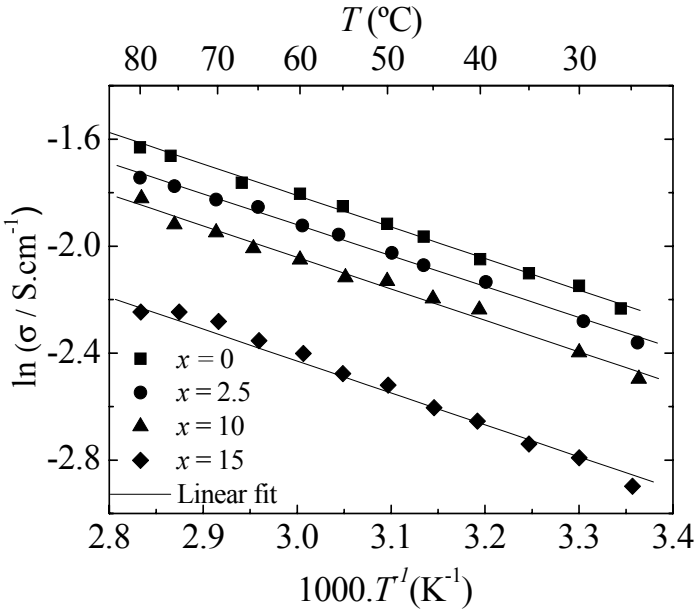

Figure 2: Arrhenius plots for cast composites NafionTiO_2.

Differential scanning calorimetry measurements for Nafion-TiO_2 composites are shown in Fig. 3. An endothermal peak ocuurring at 110ºC, associated with the glass transition temperature (Tg), was found for cast Nafion, in agreement with the Tg value for Nafion membranes (22). The addition of TiO_2 increases the Tg of Nafion, evidenced by a shift of ~20ºC to higher temperatures of the endothermal peak of composite samples. Such increase of the Tg is attributed to a lower mobility of the polymeric chains, which confers a higher mechanical stability at high temperature to the electrolyte (23).

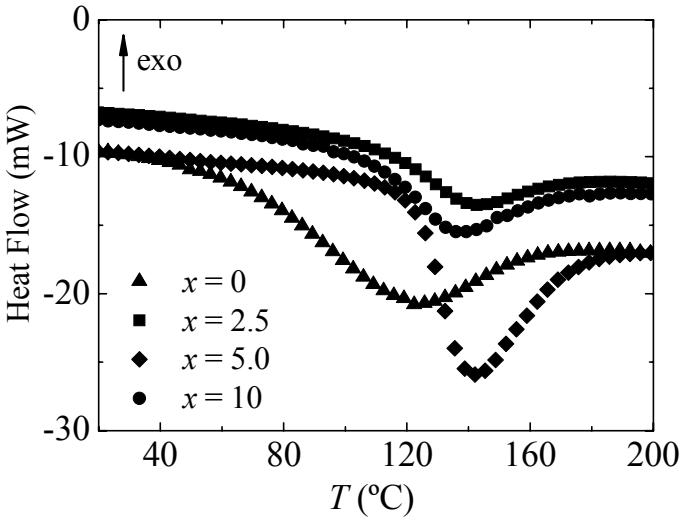

Figure 3: DSC thermograms for Nafion-TiO_2 composites.

X-ray diffraction patterns of PtSn/C electrocatalysts, displayed in Fig. 4, show peaks corresponding to the face-centered cubic (fcc) phase for platinum. Moreover, peaks at 2θ ~34 and 52° were associated to SnO_2 cassiterite phase, indicating the preferential formation of segregated platinum and tin dioxide phases for PtSn/C prepared by this methodology (24). The main crystallite sizes of the particles were calculated by Scherrer equation and a value of ~2.6 nm were obtained for all electrocatalysts.

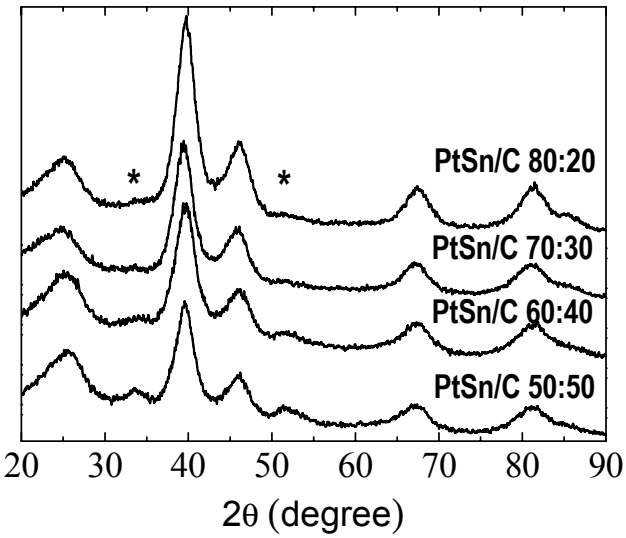

Figure 4: XRD patterns for PtSn/C electrocatalysts prepared by alcohol-reduction process. (*) corresponds to SnO_2 diffraction planes.

Fig. 5 shows cyclic voltammetry and choroamperometry measurements for PtSn/C electrocatalysts. Cyclic voltammograms (Fig. 5a) reveal that the hydrogen region of platinum is more apparent for Pt-rich electrocatalysts, i.e., PtSn/C (80:20) and commercial PtSn/C (75:25-ETEK). A suppression of the hydrogen adsorption/desorption is evidenced for the electrocatalysts with larger Sn loadings. Such a feature further supports the formation of preferential tin oxide-rich surface for these materials prepared by alcohol-reduction process. Chronoamperometry measurements (Fig. 5b) in the presence of ethanol demonstrate higher currents for all PtSn/C electrocatalysts prepared by alcohol-reduction process than that obtained for commercial one. A higher performance was observed for PtSn/C (60:40), probably, related to the presence of tin-oxygenated species that contribute to an efficient ethanol oxidation by a bifunctional mechanism.

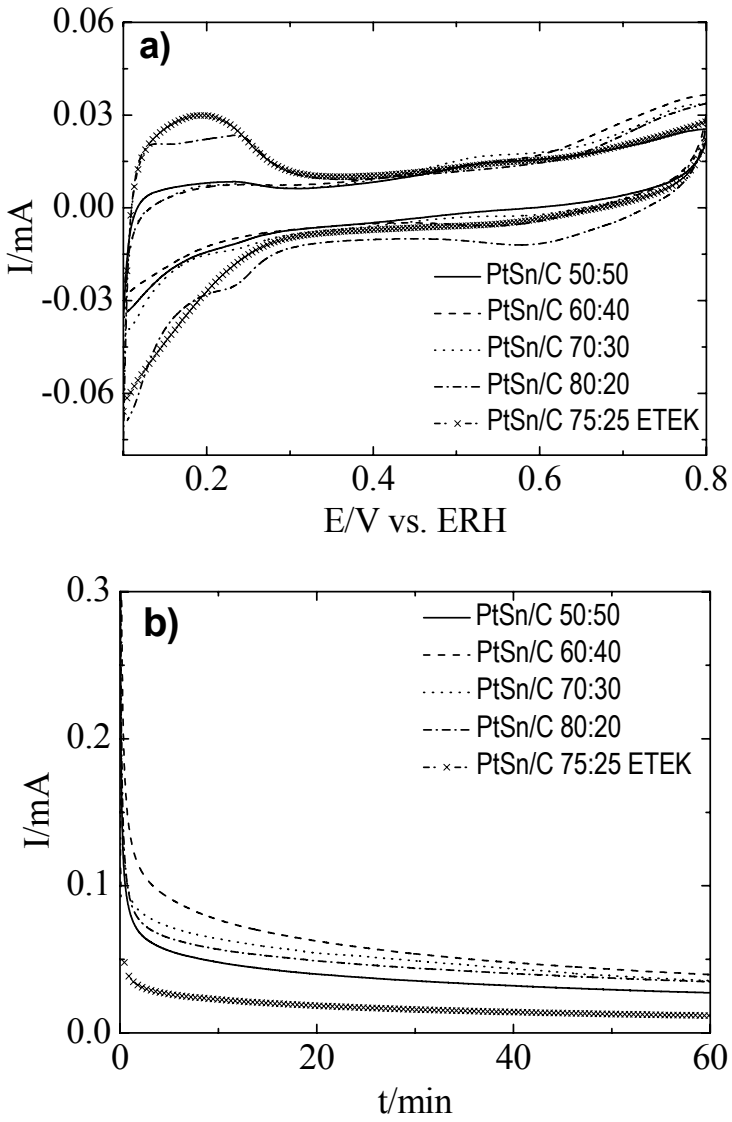

Figure 5: a) Cyclic voltammograms for PtSn/C electrocatalysts in H_2SO_4 0.5 mol L^{-1}, scan rate of 20 mV s^{-1}. b) Chronoamperometric curves for PtSn/C electrocatalysts in the presence of ethanol 1.0 mol L^{-1}. For comparison, electrochemical data for commercial PtSn/C 75:25 were included.

Both PtSn/C (60:40) and Nafion-TiO_2 10% composite were evaluated in single DEFC operating at low and high temperature (80°C and 130°C). For comparison, Pt/C and unmodified cast Nafion were tested with similar operational conditions. In the polarization data (Fig. 6) for DEFC composed with Pt/C and cast Nafion a slightly increment of performance is observed for DEFC with temperature increased from 80°C to 130°C. The maximum power density achieved was ~9 mW cm^{-2} at 130°C. An enhancement in the performance of DEFC composed by PtSn/C and Nafion-TiO_2 composite and operating at 130°C, with a maximum power density of ~50 mW cm^{-2}, was clearly evidenced when compared to the power density obtained at 80°C. Such an increase is likely to be attributed to faster ethanol oxidation reaction, lower poisoning due to CO-like species, possible crossover reduction, and a stable electrolyte (25).

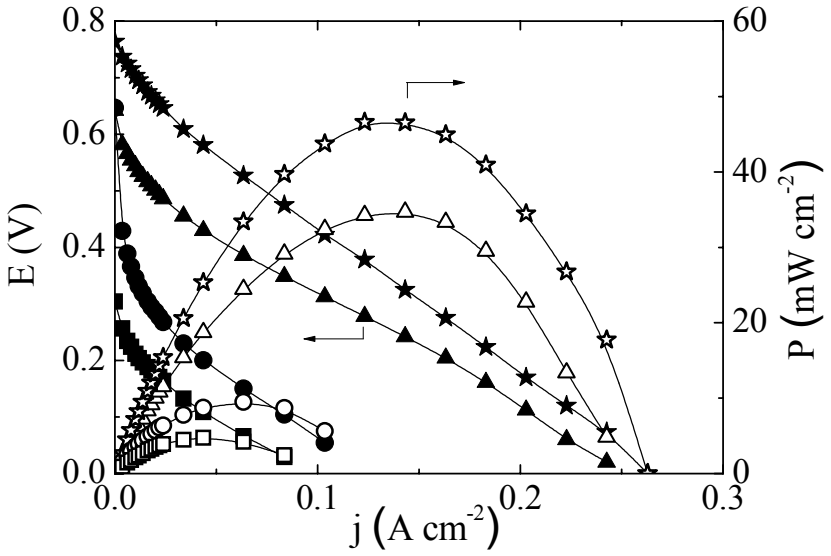

Figure 6: Polarization (solid symbols) and power density (open symbols) curves for DEFC: (■) Pt/C, cast Nafion, T_{cell}=80°C; (●) Pt/C, cast Nafion, T_{cell}=130°C; (▲) PtSn/C (60:40), Nafion-TiO_2 (*x*=10 wt%), T_{cell}=80°C; (★) PtSn/C (60:40), Nafion-TiO_2 (*x*=10%), T_{cell}=130°C. Anode fed with ethanol (2.0 mol L^{-1}, 2 mL min^{-1}) at 25°C and atmospheric pressure. Oxygen pressure = 3 atm.

Conclusion

The addition of mesoporous TiO_2 to Nafion electrolytes was found to enhance the glass transition temperature without significant decrease of both the proton conductivity and water uptake. PtSn/C electrocatalysts produced by alcohol-reduction process exhibited higher performance for ethanol oxidation than either Pt/C or commercial materials. The combined properties of the Nafion-TiO_2 composite electrolytes and PtSn/C electrocatalysts resulted in direct ethanol fuel cells operating at 130°C with a remarkably increased power density.

Acknowledgments

The authors thank the financial support of CNPq (Proc. 478970/2007-2, 306422/2007-7), FAPESP, and $PROH_2$- FINEP.

References

1. J. Larminie and A. Dicks, *Fuel Cell Systems Explained*, John Wiley & Son Ltd, Chichester, England (2000).
2. M. Linardi. *Economia e Energia*, **66**, 15 (2008).
3. D.M. dos Anjos, F Hahn, J.M. Léger, K.B. Kokoh, and G. Tremiliosi-Filho, *J. Solid State Electrochem.,* **11**, 567 (2007).
4. S. Kontou, V. Stergiopoulos, S. Song, and P. Tsiakaras, *J. Power Sources*, **171**, 1 (2007).
5. F. Colmati, E. Antolini, and E.R. Gonzalez, *J. Electrochem. Soc*., **154**, B39 (2007).
6. H.Q. Li, G.Q.Sun, L. Cao, L.H. Jiang, Q. Xin, *Electrochim. Acta*, **52**, 6622 (2007).

7. J. Ribeiro, D.M. dos Anjos, J.M. Leger, F. Hahn, P. Olivi, A.R. Andrade, G. Tremiliosi-Filho, and K.B. Kokoh, *J. Appl. Electrochem*., **38**, 653 (2008).
8. F. Colmati, E. Antolini, E.R. Gonzalez, *J. Power Sources*, **157**, 98 (2006).
9. E. Antolini, *J. Power Sources*, **170**, 1 (2007).
10. Y. Shao, G. Yin, Z. Wang, Y. Gao, *J. Power Sources*, **167**, 235 (2007).
11. K.A. Mauritz; R.B. Moore, *Chem. Rev.,* **104***,* 4535 (2004).
12. A. Saccà, A. Carbone, E. Passalacqua, A.D'Epifanio, S. Licoccia, E. Traversa, E. Sala, F. Traini, R. Ornelas, *J. Power Sources*, **152**, 16 (2005).
13. H. Uchida, Y. Ueno, H. Hagihara, M. Watanabe*, J. Electrochem. Soc*., **150**, A57 (2003).
14. K.A. Adjemian, S.J. Lee, S. Srinivasan, J. Benziger, A.B. Bocarsly, *J. Electrochem. Soc.*, **149**, A256 (2002).
15. A.K. Sahu, G. Selvarani, S. Pitchumani, P. Sridhar, and A.K. Shukla, *J. Electrochem. Soc.*, **154**, B123 (2007).
16. N.H. Jalani, K. Dunn, R. Datta, *Electrochim. Acta*, **51**, 553 (2005).
17. O. Savadogo, *J. Power Sources*, **127**, 135 (2004).
18. B.R. Matos, E.I. Santiago, F.C. Fonseca, M, Linardi, V. Lavayen, R.G. Lacerda, L.O. Ladeira, A.S. Ferlauto. *J. Electrochem. Soc.*, **154**, B1358 (2007).
19. E.V.Spinacé, A.O.Neto, T.R.R.Vasconcelos, M.Linardi. Brazilian Patent BR200304121-A.
20. D.R.M Godoi, J. Perez, and H.M. Villullas, *J. Electrochem. Soc*., **154**, B474 (2007).
21. M. Kim, C.J. Glinka, S.A. Grot, W.G. Grot*, Macromolecules*, **39** 4775 (2006).
22. S.H. Almeida, Y. Kawano, *J. Therm. Anal. Calorim*., **58**, 569 (1999)
23. V.D. Noto, R. Gliubizzi, E. Negro, G. Pace, *J. Phys. Chem. B*, **110** 24972 (2006).
24. E.V.Spinacé, L.A. Farias, M.Linardi, A.Oliveira-Neto, *Mat. Letters*, **62**, 2099 (2008).
25. E.I.Santiago, R.A.Isidoro, M.A. Dresch, B.R.Matos, M. Linardi, and F.C. Fonseca, *Electrochim. Acta*, **54**, 4111 (2009).